

# 3D MULTI-OBJECTIVE FLIGHT PATH OPTIMIZATION OF AGRICULTURAL PLANT PROTECTION UAVS BASED ON EMSDBO ALGORITHM

## 基于 EMSDBO 算法农业植保无人机三维航迹多目标优化研究

Hexia CHU<sup>\*1</sup>); Hongxing LIU<sup>2</sup>)

<sup>1</sup>) Department of Mathematics Education, Zhumadian Preschool Education College, Zhumadian, Henan, China

<sup>2</sup>) School of Mathematics and Statistics, Henan University, Kaifeng, Henan, China

\*E-mail: hexia\_chu@163.com

Corresponding author: Hexia Chu

DOI: <https://doi.org/10.35633/inmateh-72-21>

**Keywords:** agricultural UAV, patrol inspection, 3D path, multi-objective optimization

### ABSTRACT

Both cruising ability and safety should be considered in the 3D inspection path planning of agricultural unmanned aerial vehicles (UAVs). Specific to a complex working environment, the 3D inspection environment of agricultural UAVs was simulated through terrain modeling and threat modeling. First, the dynamic constraints of flight approaching rate and response time were added to the threat cost, and the 3D mission space model and flight path cost function were constructed considering the influence of UAVs' turning performance. Second, the offset estimation strategy, variable spiral search strategy, quasi-reverse learning strategy and dimension-by-dimension mutation strategy were introduced into the dung beetle optimizer (DBO) algorithm to improve the global optimization ability and convergence rate of the algorithm. By establishing a three-dimensional trajectory planning model for unmanned aerial vehicles, the trajectory planning is transformed into a multi-objective function optimization problem, and an improved algorithm is used to solve the three-dimensional trajectory planning of unmanned aerial vehicles. The fitness is evaluated by considering the objective function of trajectory cost, terrain cost, and danger level, and the trajectory planning is iteratively optimized. The results indicate that the proposed improved dung beetle algorithm for trajectory planning has lower overall cost and stability in adapting to different complex terrain environments.

### 摘要

农业无人机的三维巡检路径规划不仅要考虑续航能力，还要考虑安全性。针对复杂的作业环境，通过地形建模和威胁建模来模拟农业无人机的三维巡检环境。首先，将飞行接近率和响应时间的动态约束添加到威胁成本代价中，并考虑无人机转弯性能的影响，建立三维任务空间模型与航迹代价函数；其次，在蜣螂算法中引入偏移估计策略、变螺旋搜索策略、准反向学习策略和逐维变异策略，提高算法的全局寻优能力和收敛速度。通过建立无人机三维航迹规划模型，将航迹规划转化为多目标函数优化问题，并利用改进算法求解无人机三维航迹规划，以综合考虑航迹代价、地形代价和危险程度的目标函数评估适应度，对航迹规划迭代寻优。结果表明，所提改进蜣螂算法规划的航迹具有更低的总代价和适应不同复杂地形环境的稳定性。

### INTRODUCTION

With the development of communication technology, automatic control technology, sensing technology and artificial intelligence, the functions of unmanned aerial vehicles (UAVs) are becoming increasingly perfect. How to improve the working efficiency of UAVs and reduce their energy consumption has become a research hotspot in the field of plant protection UAVs (Gao et al., 2023). UAV route planning refers to designing a UAV flight path according to the purpose of work under the specified constraints, and the quality of the flight path is determined as per the specific purpose of work. In the military application field, military UAVs can perform various tasks such as reconnaissance and early warning, relay communication, battlefield search and rescue, and tracking and positioning. Designing a better UAV flight path can effectively avoid radar detection and improve the success rate of missions (Ling et al., 2023). In addition, UAVs have been widely used in civil applications (Xu et al., 2020).

<sup>1</sup> Chu Hexia, M.S. Stud. Eng.; <sup>2</sup> Liu Hongxing, Associate Professor. Eng.

In the logistics industry, for example, UAVs-aided autonomous distribution can effectively reduce the labour cost of logistics transportation, and the logistics transportation efficiency can be effectively improved by designing a better flight path of UAVs based on the position information of distribution sites. In the agricultural field, plant protection UAVs have exhibited such advantages as high efficiency and fast speed in the operation of mist spraying, and moreover, UAVs are capable of vertical take-off and landing in small areas and convenient spraying operations on all kinds of terrains (Qi *et al.*, 2020).

Agricultural plant protection is an important part of the modernized agricultural development, and the introduction of UAVs into agricultural plant protection can effectively meet the high-efficiency and low-cost needs in agricultural operations. The UAV technology promoted in the field of agricultural plant protection should be applied on basis of network information technology, and meanwhile, the high-efficiency, convenient and intelligent R & D concept should be adhered to, thus significantly elevating the application value of agricultural plant protection UAVs (Charalampous *et al.*, 2017). In China with a vast territory, the crop characteristics and planting patterns vary from region to region, accompanied by certain limitations in the application of traditional ground machines and tools. Under this background, the promotion of plant protection UAVs can facilitate the mechanization development of China's agriculture and elevate the overall agricultural development level of China in addition to reducing the workload of peasant households and promoting the reconstruction of the modern agricultural system.

### State of the art

The flight route design of plant protection UAVs belongs to the category of full-coverage route planning. According to the time point of route design, the full-coverage route planning algorithm is divided into two types (Zhen *et al.*, 2017). First, according to the existing environmental information including the shape and size of the target area and the distribution of obstacles in the area, a UAV flight route is designed before the UAV takes off so that the UAV can fly along the designed route. This method is referred to as the off-line route planning method. Secondly, during the flight of UAVs, the target area is scanned in real time by sensors, and the flight path of UAVs is calculated in real time based on the scanning results. This method is called the online route planning method.

Boysen *et al.* (2021) put forward a route design method for plant protection UAVs based on genetic algorithm (GA), taking route length, redundant coverage and repeated coverage as the criteria to evaluate the advantages and disadvantages of UAV routes. In addition, they put forward an operation route planning algorithm for irregular areas based on the operation direction, which could quickly plan the UAV operation route according to the specified operation direction. In the actual operation process of plant protection UAVs, the UAVs need to return to the target area several times to complete the spraying operation due to the influence of factors such as the too large target operation area and the limited drug loading and endurance of UAVs. Considering this actual situation, Zhen *et al.* (2015) proposed a path planning method of plant protection UAVs based on grid method and gravity search algorithm, taking the time spent by UAV operation as the criterion to evaluate the quality of the path, and realized the optimization of the number and position of return points. Kim *et al.* (2017) proposed an online route planning algorithm Spiral-STC based on Spanning Tree Coverage (STC), which obtained the surrounding environment information through sensors and generated local maps, and obtained effective grids and obstacle grids through grid division of local maps. This method can ensure that all effective grids are covered, without repeated coverage. Due to too many turns of the designed route, however, the energy consumption cost is increased, and in addition, missing coverage results from the inaccurate grid division. Ham *et al.* (2018) put forward an improved Spiral-STC algorithm, which added outer ring routes to the original Spiral-STC algorithm, which can effectively improve the coverage of routes. Choi *et al.* (2021) added a new map coordinate allocation method on this basis, and redistributed the coordinates by analysing the historical coordinate data of sensors, which can effectively reduce the number of turns of the route. Common path planning algorithms include A\* algorithm (Ha *et al.*, 2016), Probabilistic Roadmap (PRM) algorithm (Lu *et al.*, 2016), rapidly expanding random tree (RRT) algorithm (Agatz *et al.*, 2018), artificial potential field method (Carlsson *et al.*, 2018), Dijkstra method (Kitjacharoenchai *et al.*, 2019) and so on. Despite the quite mature mathematical theories, the traditional path planning methods can easily fall into the local optimal solution when solving the multi-objective 3D path planning problem of UAVs. With the development of random search theory, many emerging swarm intelligence algorithms have been successfully applied to path planning problems in recent years, such as traditional particle swarm optimization (Das *et al.*, 2021), as well as newly proposed artificial bee colony algorithm, grey wolf algorithm (Roberti *et al.*, 2021).

At present, the main problems of UAVs' 3D path planning lie in the rationality and safety of modeling and the solving accuracy and global optimization ability of algorithms in complex geographical environments.

In terms of modeling improvement, *Kim et al. (2019)* divided sub-paths according to the number of hazard sources and the distance from the hazard sources, and respectively calculated the threat cost of the sub-paths by threat weight factors. *Wang et al. (2017)* adopted a two-level path planning method, established a Markov decision process at the bottom to control the movement of the UAV along the route, divided the UAV control into different discrete actions, and set a reward function to reduce the risk of collision. In the modeling process of the above research, when considering obstacle avoidance, the distance from the obstacle is often used as the judgment condition (*Ulmer et al., 2018*), but in practice, the manoeuvrability and turning performance of UAVs should be considered comprehensively, so as to plan a safer and more practical path (*Zhang et al., 2021*). In terms of algorithm improvement, *Otto et al. (2018)* proposed a particle swarm optimization algorithm with spherical vectors, which introduced the elevation angle and azimuth angle of spherical coordinate vectors to achieve performance constraints on the pitch angle and steering angle of UAVs, significantly reducing the search space. Given the large search space and many constraints in the 3D path planning problem and despite the ability to help improve the path planning quality of algorithms to some extent, the above improvement is restricted by the characteristics of traditional algorithms themselves.

To sum up, although the multi-objective path planning problem of UAVs has been investigated by many scholars, the multi-modal and multi-objective characteristics of UAV paths have not been considered in most cases. To solve the above problems, a 3D UAV path planning model under complex environments was established in this study with UAVs' fuel consumption and threat as the optimization objectives. In the aspect of algorithm improvement, the strategy improvement was performed based on the dung beetle optimizer (DBO), and an enhanced multi-strategy dung beetle optimizer (EMSDBO) was proposed, followed by simulation verification on the standard function and the established 3D flight path model of agricultural plant protection UAVs. The experimental results reveal that the improved algorithm can plan the better UAV flight path on the premise of ensuring the rapid and safe optimization.

## MATERIALS AND METHODS

### Environment Modeling

Environment modeling is the first step of UAV path planning, which usually includes terrain modeling and threat modeling. Obstacles are a key factor affecting the safe flight of agricultural drones. When performing inspection tasks, in addition to avoiding terrain obstacle, it is also necessary to consider detecting obstacle. This article mainly considers the obstacle caused by signal interference in reconnaissance environments, which generally involve obstacle such as radar, electromagnetic, and artillery. These obstacles are simulated using cylinders. Different from the function-based simulation, different elevation values were assigned to different positions in the 2D plane using digital elevation information so as to realize the terrain undulation. In addition, digital elevation model (DEM) has been commonly used to establish 3D environments. After the DEM data of a region was acquired, the simulation modeling of 3D terrains could be implemented via MATLAB to realize the digital simulation of terrain surfaces. When executing a reconnaissance mission, UAVs need to consider the detection threat in addition to evading the terrain threat. In this study, the threat brought by signal interference under the flight environment of agricultural plant protection UAVs was mainly considered. For the sake of simplification, the threatened area was simplified into a cylinder (*Chen et al., 2023*), expressed by the following formula:

$$E(\epsilon) = \left( \frac{x - x_0}{a} \right)^{2d} + \left( \frac{y - y_0}{b} \right)^{2e} + \left( \frac{z - z_0}{c} \right)^{2f} \quad (1)$$

In Equation (1),  $(x_0, y_0, z_0)$  represents the coordinates of the interference enter,  $a=b$ ,  $d=e=1$ ,  $f>1$ ;  $E(\epsilon)=1$  stands for the surface of the cylinder.

### Path Planning Model

The path of UAVs can be regarded as a line segment connected by a series of coordinate points. Therefore, the path is coded by means of real number coding, as follows:

$$(x_1, x_2, \dots, x_n, y_1, y_2, \dots, y_n, z_1, z_2, \dots, z_n) \quad (2)$$

where  $x_i (i=1, 2, \dots, n)$  represents the x-coordinate of the  $i$ -th flight path point;  $y_i (i=1, 2, \dots, n)$  and  $z_i (i=1, 2, \dots, n)$  stand for the y-coordinate and z-coordinate of the  $i$ -th flight path point, respectively;  $n$  denotes the number

of path nodes. The path planning model of UAVs contains terrain constraints and turning angle constraints. Terrain constraints are expressed as follows:

$$h(x_i, y_i) + z_{\min} < z_i < z_{\max}, i = 1, 2, \dots, n \tag{3}$$

where  $h(x_i, y_i)$  is the terrain height corresponding to 2D terrain coordinates;  $Z_{\min}$  and  $Z_{\max}$  represent the minimum and maximum safety flight heights of UAVs, respectively. According to reference *Radmanesh et al. (2015)* Other constraints such as the minimum and maximum path lengths and the maximum turning angle can be expressed as follows:

$$\theta_i \leq \theta_{\max}, i = 1, 2, \dots, n \tag{4}$$

$$L_i \geq L_{\min}, i = 1, 2, \dots, n \tag{5}$$

$$\sum_{i=1}^n L_i < L_{\max}, i = 1, 2, \dots, n \tag{6}$$

where  $\theta_i$  is the turning angle of the  $i$ -th path point;  $\theta_{\max}$  stands for the maximum turning angle;  $L_i$  is the length of the  $i$ -th path segment;  $L_{\min}$  is the minimum path length;  $L_{\max}$  is the maximum path length.

In this study, fuel consumption and threat were taken as two optimization objectives, which were in conflict under some circumstances, e.g., the shorter the path, the greater the threat.

(1) Fuel consumption. Generally speaking, a short path length means short flight time and less fuel consumption. In this study, fuel consumption refers to the fuel consumed by the UAV during the flight from the starting point to the target point.  $f_{oil}$  was set as the fuel consumption cost. Assuming that the UAV flew at a constant speed, the fuel consumption was then directly proportional to the path length. Hence, the fuel consumption  $f_{oil}$  could be calculated as below:

$$f_{oil} = \alpha \sum_{i=1}^n L_i = \alpha \sum_{i=1}^n \sqrt{(x_i - x_{i-1})^2 + (y_i - y_{i-1})^2 + (z_i - z_{i-1})^2} \tag{7}$$

where  $\alpha$  is the fuel consumption coefficient.

(2) Obstacles. In this study, detection obstacle and height obstacle were mainly considered (*Chen et al., 2023; Lebedeva et al., 2022; Liu et al., 2021*). A total of  $m$  detection obstacles are set, the protection centre coordinate of the  $k$  ( $k=1, 2, \dots, m$ )-th detection threat is  $C_k$ , and the radius of the threat is  $R_k$ ; when the UAV flies from the path node  $W_i$  to node  $W_{i+1}$ , the straight-line distance from  $C_k$  to  $W_i, W_{i+1}$  is  $d_k$ , as shown in Fig. 1.

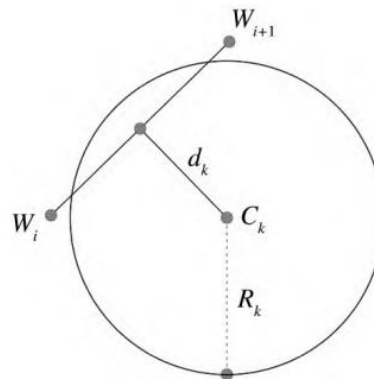


Fig. 1- Definition of detection obstacle

In this case, the detection threat value of UAVs is inversely proportional to its distance  $d_k$ . Therefore, the detection threat  $f_{detect}$  can be calculated as follows:

$$f_{detect} = \sum_{i=1}^n \sum_{k=1}^m T_{i,k} \tag{8}$$

$$T_{i,k} = \begin{cases} 0, & d_k \geq R_k \\ R_k / d_k, & 0 < d_k < R_k \\ \infty, & d_k = 0 \end{cases} \tag{9}$$

where  $T_{i,k}$  denotes the detection threat value borne by the UAV from the  $k$ -th interference centre on the  $i$ -th path segment. The greater the flight height of the UAV, the higher the probability for the UAV to be discovered by the enemy. Hence, the flight height is also one of the obstacle to be considered in this study. In 3D maps, the UAV should keep flying at an average safety height as much as possible, and meanwhile, prevent the collision with the terrain environment. Hence, the height threat  $f_{high}$  can be calculated as below:

$$f_{high} = \sum_{i=1}^n H_i \tag{10}$$

$$H_i = \begin{cases} \left| z_i - \frac{z_{max} + z_{min}}{2} \right|, & h(x_i, y_i) + z_{min} < z_i < z_{max} \\ \infty, & \text{else} \end{cases} \tag{11}$$

where  $H_i$  stands for the height threat of the UAV in the  $i$ -th path segment. Therefore, the threat  $f_{threat}$  of the UAV can be expressed as follows:

$$f_{threat} = f_{detect} + f_{high} \tag{12}$$

According to the above analysis, the 3D path planning model for the UAV can be expressed as below:

$$F = [\min(f_{oil}), \min(f_{threat})]^T \tag{13}$$

$$s.t. \begin{cases} h(x_i, y_i) + z_{min} < z_i < z_{max}, i = 1, 2, \dots, n \\ \theta_i \leq \theta_{max}, i = 1, 2, \dots, n \\ L_i \geq L_{min}, i = 1, 2, \dots, n \\ \sum_{i=1}^n L_i \geq L_{max}, i = 1, 2, \dots, n \end{cases} \tag{14}$$

where  $F$  is the objective vector, which is a constrained double-objective minimization-type optimization problem. In this study, two objective functions—fuel consumption cost and threat cost—were designed when establishing the multi-objective 3D path optimization model of agricultural plant protection UAVs, aiming to realize the optimal overall inspection path. By fully considering the advantages and disadvantages of agricultural plant protection UAVs in patrol inspection, the relationship between the two objective functions was coordinated, and the 3D path optimization of such UAVs was, in essence, the trade-off selection process of participants. Different 3D paths of agricultural plant protection UAVs were selected by assigning different weights to different optimization objectives. In the solving process based on heuristic algorithms, the values of the two objective functions for each generation of individuals could be acquired, and the two objective functions were respectively subjected to uniform dimensionality and quantification as per the following formulas:

$$F_{oil}^* = \frac{f_{oil} - \min f_{oil}}{\max f_{oil} - \min f_{oil}} \tag{15}$$

$$F_{threat}^* = \frac{f_{threat} - \min f_{threat}}{\max f_{threat} - \min f_{threat}} \tag{16}$$

The two objective functions with the unified dimension were weighted and summed according to the specified weights and transformed into a single-objective model for solving. The single-objective function is expressed as below:

$$\min F^* = \alpha_1 F_{oil}^* + \alpha_2 F_{threat}^* \tag{17}$$

where  $\alpha_i$  is the weight of the objective function,  $\alpha_i \in [0, 1]$  and  $\alpha_1 + \alpha_2 = 1$ .

**Algorithm Design**

In this study, the DBO algorithm was improved and the improved algorithm was applied to the established simulation scenario for path planning. The idea of the DBO algorithm is mainly based on four behaviours of dung beetles, namely, ball rolling, reproduction, foraging and stealing. Among them, the ball rolling behaviour is divided into two modes: with and without obstacles (Sui et al., 2023), and the position updating in case of no obstacles in the forward direction is displayed in the following formula:

$$x_i^{t+1} = x_i^t + \alpha \times k \times x_i^{t-1} + b \times \Delta x \tag{18}$$

$$\Delta x = |x_i^t - X^w| \tag{19}$$

where  $t$  represents the current iteration number,  $x_i^t$  is the position of the  $i$ -th dung beetle at the  $t$ -th iteration,  $k$  is the deflection factor,  $b$  is a constant value within (0,1), and  $\alpha$  is a natural coefficient with a value of -1 or 1, where 1 means no deviation and -1 means the deviation from the original direction.  $x^w$  is the worst position of dung beetle in all the solutions and  $\Delta x$  is used to simulate the intensity change of light. When there is an obstacle in the forward direction, the position updating formula is shown in the following Formula (20):

$$x_i^{t+1} = x_i^t + \tan(\theta) |x_i^t - x_i^{t-1}| \tag{20}$$

The rolling direction is only considered within  $[0, \pi]$ . If  $\theta$  is equal to  $0, \pi/2$  or  $\pi$ , the position will not be updated. In the breeding behaviour, a dynamic boundary selection strategy is proposed to represent the spawning area, as shown in the following Formulas (21) and (22):

$$Lb^* = \max(X^* \times (1 - R), Lb) \tag{21}$$

$$Ub^* = \min(X^* \times (1 + R), Ub) \tag{22}$$

Among them:  $X^*$  represents the current local optimal position,  $Lb^*$  and  $Ub^*$  respectively stand for the upper and lower bounds of the breeding area, and  $R=1-t/T_{max}$ , in which  $T_{max}$  means the maximum number of iterations, and  $Lb$  and  $Ub$  denote the upper and lower bounds of the optimization problem, respectively. The spawning position will change dynamically, as seen in the following Formula (23):

$$B_i^{t+1} = X^* + b_1 \times (B_i^t - Lb^*) + b_2 \times (B_i^t - Ub^*) \tag{23}$$

Among them:  $B_i^t$  is the spawning position of the  $i$ -th female dung beetle at the  $t$ -th iteration,  $b_1$  and  $b_2$  represent two independent random vectors with a size of  $1 \times D$ , and  $D$  is the dimension of the optimization problem. The optimal foraging area in the foraging behaviour is also dynamically updated, expressed by the following Formulas (24) and (25).

$$Lb^b = \max(X^b \times (1 - R), Lb) \tag{24}$$

$$Ub^b = \min(X^b \times (1 + R), Ub) \tag{25}$$

where  $X^b$  represents the global optimal position, and  $Lb^b$  and  $Ub^b$  respectively represent the lower and upper limits of the optimal foraging area. The individual position updating is shown in the following Formula (26):

$$x_i^{t+1} = x_i^t + C_1 \times (x_i^t - Lb^b) + C_2 \times (x_i^t - Ub^b) \tag{26}$$

Where  $C_1$  represents a random number that obeys a normal distribution and  $C_2$  represents a random vector within  $(0,1)$ . The individual position update of stealing behaviour is shown in the following Formula (27):

$$x_i^{t+1} = X^b + S \times g \times (|x_i^t - X^*| + |x_i^t - X^b|) \tag{27}$$

Where  $X^b$  is the best food source,  $g$  is a random vector with a size of  $1 \times D$ , which follows a normal distribution, and  $S$  represents a constant value.

**Improved Optimization Strategy**

In order to further improve the performance in 3D path planning of UAVs, the following improvement strategy was designed for the DBO algorithm.

(1) Offset estimation strategy. In this study, an offset estimation strategy (Chen et al., 2023) was proposed, the mutual relationship between individuals was expressed via a probability model, the probability distribution model was calculated using the current dominant population, the evolutionary direction of the population was led, and new sub-populations were generated based on the sampling of the probability distribution model, followed by continuous iterations until obtaining the optimal solution. The mathematical models for the offset estimation strategy are displayed in Formulas (28), (29), (30) and (31):

$$x_i^{t+1} = \frac{(x^b + x_{mean}^t + x_i^t)}{3} + y, y \sim N(0, Cov(i)) \tag{28}$$

$$Cov(i) = \frac{1}{pop/2} \sum_{i=1}^{pop/2} (x_i^{t+1} - x_{mean}^t) \times (x_i^t - x_{mean}^t)^T \tag{29}$$

$$x_{mean}^t = \sum_{i=1}^{pop/2} \omega_i \times x_i^t \tag{30}$$

$$\theta_i = \frac{\ln(pop/2 + 0.5) - \ln(i)}{\sum_{i=1}^{pop/2} (\ln(pop/2 + 0.5) - \ln(i))} \tag{31}$$

where  $x_{mean}^t$  represents the weighted average of the dominant population,  $pop$  is the population size,  $\theta_i$  stands for the weight coefficient arranged according to the descending order of the fitness value in the dominant population, and  $Cov(i)$  is the weighted covariance matrix. In the process of updating, both the global optimal individual information and the population position and its own information are considered, which is helpful to keep the population diversity of the algorithm.

(2) The spiral search formula of the traditional whale optimization algorithm is a fixed spiral line. In order to dynamically adjust the spiral shape during the search with the iteration and strengthen the ability of the

algorithm to explore unknown areas, an improved variable spiral search strategy was proposed in this study, with the specific mathematical formulas shown in (32) and (33):

$$\beta = e^{Bt} \times \cos(2\pi B) \tag{32}$$

$$l = e^{4 \cos\left(\frac{1-t}{t_{\max}} + 1\right)\pi} \tag{33}$$

Where  $B$  is a random number evenly distributed from 0 to 1,  $l$  changes gradually with the increase in the number of iterations, and the change in the spiral line is controlled by a cosine function. As iterations proceed, the spiral line gradually changes from a large one to a small one. In the early stage, the algorithm searches the target in a large spiral shape, trying to find better individuals as much as possible and enhance the algorithm's global search ability (according to reference *Li et al. 2023*). In the later stage, ineffective search is reduced, and the target is searched in a small spiral shape to improve the algorithm optimization accuracy and convergence efficiency. The modified foraging, reproduction and stealing formulas for dung beetles are displayed in the following Formulas (34), (35) and (36):

$$x_i^{t+1} = x^* + \beta_1 \times (x_i^t - Lb^*) + \beta_2 \times (x_i^t - Ub^*) \tag{34}$$

$$x_i^{t+1} = x_i^t + \beta_3 \times (x_i^t - Lb^b) + \beta_4 \times (x_i^t - Ub^b) \tag{35}$$

$$x_i^{t+1} = x^b + \beta_5 \times g \times (|x_i^t - x^*| + |x_i^t - x^b|) \tag{36}$$

$Lb^b$  and  $Ub^b$  represent the lower limit and upper limit of the optimal feeding area, respectively.  $Lb^*$  and  $Ub^*$  represent the lower and upper limits of the spawning area, respectively.  $\beta_1$  and  $\beta_2$  represent two independent random vectors of size  $1 \times D$ , and  $D$  represents the dimension of the optimization problem.  $\beta_3$  represents a random number that follows a normal distribution,  $\beta_4$  represents a random vector belonging to (0,1), and  $\beta_5$  represents a constant value.

(3) Quasi-reverse learning strategy. In the DBO algorithm, the position updating process depends too much on the dominant individuals, which leads to the prematurity of the population. To solve this problem, an adaptive quasi-reverse learning strategy was put forward in this study. The quasi-reverse learning strategy is a variant of the reverse learning strategy, which can evade the low accuracy caused by the excessive position conversion of traditional reverse learning, and meanwhile, can relatively expand the search space and accelerate population convergence, as shown in Formula (37):

$$x_i^{qp} = rand\left(\frac{Lb + Ub}{2}, Lb + Ub - x_i\right), \quad i = 1, 2, \dots, pop \tag{37}$$

In addition, the quasi-reverse learning strategy is used for all individuals as iterations proceed, and many useless searches will appear, which increases the calculation cost and is not good for algorithm convergence. Hence, the linear population reduction strategy was proposed in this study to gradually reduce the number of individuals adopting the quasi-reverse learning strategy with the proceeding of iterations, specifically as seen in Formula (38):

$$pop' = round\left(\frac{(pop_{\min} - pop_{\max}) \cdot t}{M} + pop_{\max}\right) \tag{38}$$

where  $pop'$  represents the population size adopting the quasi-reverse learning strategy, and  $pop_{\min}$  and  $pop_{\max}$  stand for the maximum and minimum population sizes, respectively.

(4) Dimension-by-dimension mutation strategy

In order to enhance the ability of the algorithm to get rid of the local optimum, the dimension-by-dimension mutation strategy was adopted for the obtained optimal individuals after the ending of each iteration, and the best individual was retained by using the greedy strategy. In this stage, Gaussian mutation or Cauchy strategy was applied to each dimension of the optimal individual, specifically as seen in Formulas (39) and (40):

$$x_{new}^b(j) = \begin{cases} x^b(j) + randn \times \cos\left(\frac{\pi t}{2t_{\max}}\right) \times (x^b(j) - x^{random}(j)), & \text{if } rand < 0.5 \\ x^b(j) + cauchy \times x^b(j), & \text{else} \end{cases} \tag{39}$$

$$x^b(j) = \begin{cases} x_{new}^b(j), & \text{if } f(x_{new}^b) < f(x^b) \\ x^b(j), & \text{if } f(x_{new}^b) \geq f(x^b) \end{cases} \tag{40}$$

where  $x^b(j)$  is the  $j$ -th dimension of the optimal individual.

**Simulation Experiment**

First, the improved EMSDBO algorithm was compared with other optimization algorithms to verify the superiority of the improved algorithm; then, different improvement strategies were compared, and the effectiveness of different improvement strategies was analysed; finally, the EMSDBO algorithm was subjected to 3D path planning simulation with other path planning algorithms in the established path planning model of agricultural plant protection UAVs under the same conditions, aiming to verify the effectiveness of this algorithm in path planning.

The real terrain data were acquired by reading DEM maps, which corresponded to the mountainous terrain in real environments. In this study, the DEM data were obtained from ALOSPALSAR database, and elevation points were acquired according to DEM and evenly discretized in the 100\*100 coordinate space. X-coordinate represents the east longitude,  $x \in [0,100]$ , y-coordinate stands for the north latitude,  $y \in [0,100]$ , and z-coordinate denotes the real height of each coordinate point. The simulation experimental parameters and constraints are set as seen in Table 1.

**Table 1**

**Settings of simulation experimental parameters**

Experimental parameter	Set value	Experimental parameter	Set value	Experimental parameter	Set value
m	15	T	10	ganum	100
$\phi_{max}$	45°	$\varphi_{max}$	45°	$h_{max}$	1000 m
$l_{min}$	30m	$h_{min}$	0 m	$t_{min}$	2s
$v_1$	15m/s	$v_2$	10 m/s	$v_3$	5 m/s
$\phi_0$	30°	$\varphi_0$	30°	saft	1000 m
$\alpha_1$	0.6	$\alpha_2$	0.4	$w_1$	0.4
$w_2$	0.2	$w_3$	0.2	$w_4$	0.2

**RESULTS**

In the experiment, the coordinates of the starting point and the target point of the planned path for agricultural plant protection UAVs were (1,1,100) and (100,100,100), respectively. In order to display the planned 3D path for agricultural plant protection UAVs more intuitively and accurately, in the above calculation example, the 3D flight path of the UAVs was displayed through a 3D coordinate system in MATLAB 2014b. Then, the model was solved respectively using the DBO algorithm, the variable spiral search strategy-based DBO (SDSO) algorithm and the enhanced multi-strategy DBO (EMSDBO) algorithm. The convergence curves of the three algorithms are exhibited in Fig. 2, and the paths of agricultural plant protection UAVs obtained by the three algorithms are as shown in Fig. 3.

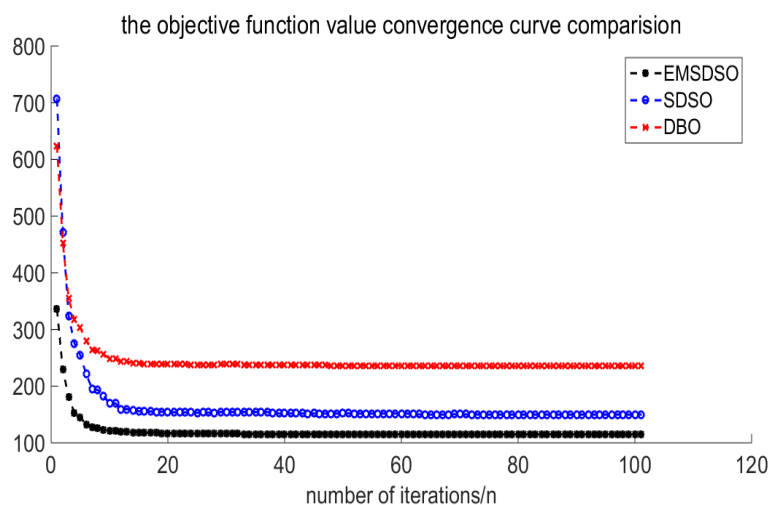


**Fig. 2 - Convergence curves of three algorithms**

It could be known from Fig. 2 that both the convergence rate and the objective function value of the EMSDBO algorithm were better than those of the DBO algorithm and SDSO algorithm.



The concepts of flight approaching rate and response time were introduced in the EMSDBO algorithm. Compared with the DBO and SDBO algorithms, the average minimum response time of the EMSDBO algorithm was 3.27 s, which was sufficient and reasonable, accompanied by relatively moderate flight distance and threat cost. This reflects that the influence of the flight approaching rate is taken into account and the planned path will be more reasonable and safer and accord with the actual situation by setting the suitable minimum response time, adding the dynamic constraint to the approaching distance and fully considering the manoeuvrability and turning performance of UAVs.

Therefore, it could be seen by comparing the experimental results that the EMSDBO algorithm proposed in this study can effectively avoid obstacle and plan the actually optimal flight path when applied to 3D path planning of plant protection UAVs. This process successfully shortens the search time during path planning using the algorithm and the length of the planned path, thus verifying the effectiveness and progressiveness of the EMSDBO algorithm.

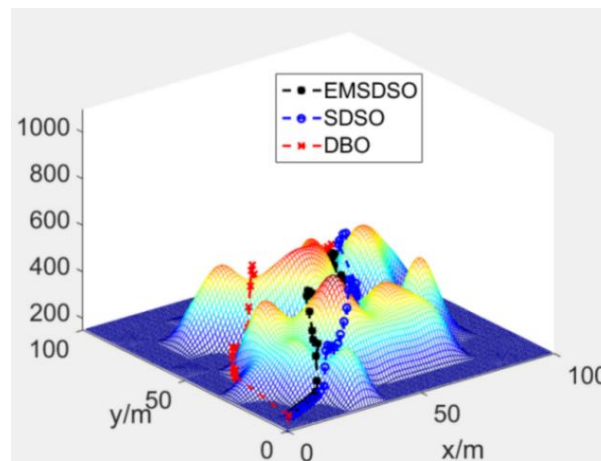


Fig. 3 - Paths of agricultural plant protection UAVs obtained by three algorithms

## CONCLUSIONS

In order to effectively solve the 3D path planning problem of UAVs, the 3D UAV path planning models of two different scenarios were proposed first; second, the fuel consumption and threat of UAVs were set as the optimization objectives; finally, the EMSDBO algorithm was proposed. Specifically, multiple improvement strategies such as the offset estimation strategy, variable spiral search strategy, adaptive quasi-reverse learning strategy and hybrid mutation strategy were introduced based on DBO to enhance the population diversity and increase the algorithm global optimization ability and convergence rate. The simulation experimental results manifest that compared with the situation only considering the distance from the hazard source, the generated flight path will be safer and reasonable if the influence of the flight approaching rate and turning rate is taken into account; the improved algorithm exhibits stronger global search ability and can stably plan a feasible and safe flight path. The follow-up study will be carried out from two aspects: the real-time 3D path replanning of UAVs under dynamic environments will be implemented on basis of this study, and meanwhile, the collaborative path planning method under the condition of UAV groups will be explored.

## REFERENCES

- [1] Agatz N, Bouman P, Schmidt M., (2018), Optimization approaches for the traveling salesman problem with drone, *Transportation Science*, vol. 52, no. 4, ISSN 0041-1655, pp. 965-981, United States;
- [2] Boysen N, Fedtke S, Schwerdfeger S., (2021), Last-mile delivery concepts: a survey from an operational research perspective, *OR Spectrum*, vol. 43, ISSN 0171-6468, pp. 1-58, Germany;
- [3] Carlsson J G, Song S., (2018), Coordinated logistics with a truck and a drone, *Management Science*, vol. 64, no. 9, ISSN 0025-1909, pp. 4052-4069, United States;
- [4] Charalampous K., Kostavelis I., and Gasteratos A., "Thorough robot navigation based on SVM local planning," *Robotics and Autonomous Systems*, vol. 70, pp. 166–180, 2017.
- [5] Chen X, Huang Y, Fan Q., (2023), Three-dimensional Path Planning of UAV Based on Multimodal Multi-objective Evolutionary Algorithm (基于多模态多目标进化算法的无人机三维路径规划), *Fire Control & Command Control*, vol. 48, no. 11, ISSN 1002-0640, pp. 32-40, China;

- [6] Choi Y, Schonfeld P M., (2021), A Comparison of optimized deliveries by drone and truck, *Transportation Planning and Technology*, vol. 44, no. 3, ISSN 0308-1060, pp. 319-336, England;
- [7] Das D, Sewani R, Wang J, Tiwari M., (2021), Synchronized truck and drone routing in package delivery logistics, *IEEE Transactions on Intelligent Transportation Systems*, vol. 22, no. 9, ISSN 1524-9050, pp. 5772-5782, United States;
- [8] Deng, L.; Chen, H.; Zhang, X.; Liu, H. Three-Dimensional Path Planning of UAV Based on Improved Particle Swarm Optimization. *Mathematics* 2023, 11, 1987. <https://doi.org/10.3390/math11091987>
- [9] Gao M, Han J, Feng X., (2023), Task allocation and service path optimization for plant protection drone based on agricultural service platforms (基于农服平台的植保无人机任务分配与路径优化), *Journal of Huazhong Agricultural University*, vol. 42, no. 3, ISSN 1000-2421, pp. 250-259, China;
- [10] Ham A M., (2018), Integrated scheduling of m-truck, m-drone, and m-depot constrained by time-window, drop-pickup, and m-visit using constraint programming, *Transportation Research Part C: Emerging Technologies*, vol. 91, ISSN 0968-090X, pp. 1-14, England;
- [11] Kitjacharoenchai P, Ventresca M, Moshref M, Lee S, Tanchoco J, and Brunese P., (2019), Multiple traveling salesman problem with drones: mathematical model and heuristic approach, *Computers & Industrial Engineering*, vol. 129, ISSN 0360-8352, pp. 14-30, England;
- [12] Kim S, Moon I., (2019), Traveling salesman problem with a drone station, *IEEE Transactions on Systems, Man, and Cybernetics: Systems*, vol. 49, no. 1, ISSN 2168-2216, pp. 42-52, United States;
- [13] Kim S J, Lim G J, Cho J, Côté M J., (2017), Drone-aided healthcare services for patients with chronic diseases in rural areas, *Journal of Intelligent and Robotic Systems*, vol. 88, no. 1, ISSN 0921-0296, pp. 163-180, Netherlands;
- [14] Lebedeva V.V., Lebedev I.V., Algorithms for Calculating the Trajectory of Unmanned Aerial Vehicles for Solving Agricultural Problems, *Agricultural Machinery and Technologies*, vol. 16, No. 3, 2022
- [15] Ling B, Zhang S., (2023), Application Status and development suggestions of UAV for agricultural plant protection in Xinjiang (新疆农业植保无人机的应用现状及发展建议), *China Plant Protection*, vol. 43, no. 4, ISSN 1672-6820, pp. 87-89, China;
- [16] Li Y, Sun K, Yao Q, et al. (2023), A dual-optimization wind speed forecasting model based on deep learning and improved dung beetle optimization algorithm [J]. *Energy*: 129604.
- [17] Lu Z., (2016), Modeling of yard congestion and optimization of yard template in container ports, *Transportation Research Part B: Methodological*, vol. 90, ISSN 0191-2615, pp. 83-104, England;
- [18] Otto A, Agatz N, Campbell J, Golden B, Pesch E., (2018), Optimization approaches for civil applications of unmanned aerial vehicles (UAVs) or aerial drones: a survey, *Networks*, vol. 72, no. 4, ISSN 1097-0037, pp. 411-458, England;
- [19] Panagiotis Radoglou-Grammatikis, Panagiotis Sarigiannidis, Thomas Lagkas, Ioannis Moscholios, A compilation of UAV applications for precision agriculture, *Computer Networks*, Volume 172, 2020, 107148, ISSN 1389-1286, <https://doi.org/10.1016/j.comnet.2020.107148>.
- [20] Roberti R, Ruthmair M., (2021), Exact methods for the traveling salesman problem with drone, *Transportation Science*, vol. 55, no. 2, ISSN 0041-1655, pp. 315–335, United States;
- [21] Radmanesh, Mohammadreza & Kumar, Manish & Nemat, Alireza & Sarim, Mohammad. (2015). Dynamic optimal UAV trajectory planning in the National Airspace System via mixed integer linear programming. *Proceedings of the Institution of Mechanical Engineers Part G Journal of Aerospace Engineering*. 230. 10.1177/0954410015609361.
- [22] Samaniego F, Sanchis J, Rodriguez S G-N, Simarro R., (2019). Smooth 3D Path Planning by Means of Multiobjective Optimization for Fixed-Wing UAVs, *Electronics* 9(1): 51.
- [23] Shubhani Aggarwal, Neeraj Kumar, (2020). Path planning techniques for unmanned aerial vehicles: A review, solutions, and challenges, *Computer Communications*, Volume 149, Pages 270-299, ISSN 0140-3664, <https://doi.org/10.1016/j.comcom.2019.10.014>.
- [24] Sui D, Yang Z, Ding S, Zhou B., (2023), Three-dimensional path planning of UAV based on EMSDBO algorithm(基于 EMSDBO 算法的无人机三维航迹规划), *Systems Engineering and Electronics*, ISSN 1001-506X, <https://link.cnki.net/urlid/11.2422.TN.20231205.1202.016>, China;
- [25] Tsouros, D.C.; Bibi, S.; Sarigiannidis, P.G. A Review on UAV-Based Applications for Precision Agriculture. *Information* 2019, 10, 349. <https://doi.org/10.3390/info10110349>

- [26] Ulmer M W, Thomas B W., (2018), Same-day delivery with heterogeneous fleets of drones and vehicles, *Networks*, vol. 72, no. 4, ISSN 1097-0037, pp. 475-505, England;
- [27] Wang X, Poikonen S, Golden B., (2017), The vehicle routing problem with drones: several worst-case results, *Optimization Letters*, vol. 11, no. 4, ISSN 1862-4472, pp. 679-697, Germany;
- [28] Wang Y, Wang S. (2020). UAV path planning based on improved particle swarm optimization[J]. *Computer Engineering & Science*, 42(09): 1690.
- [29] Xu L, Yang Z, Huang Z, Ding W., (2020), Route planning method for plant protection Unmanned Aerial Vehicles combined with hybrid particle swarm optimization(结合混合粒子群算法的植保无人机航线设计方法), *Journal of Chinese Computer Systems*, 1000-1220, vol. 41, no. 9, ISSN 1000-1220, pp. 1826-1832, China;
- [30] Yang, Y.; Xiong, X.; Yan, Y. UAV Formation Trajectory Planning Algorithms: A Review. *Drones* 2023, 7, 62. <https://doi.org/10.3390/drones7010062>
- [31] Yiheng Liu, Honglun Wang, Jiaxuan Fan, Jianfa Wu, Tiancai Wu, Control-oriented UAV highly feasible trajectory planning: A deep learning method, *Aerospace Science and Technology*, Volume 110,2021, 106435, ISSN 1270-9638, <https://doi.org/10.1016/j.ast.2020.106435>.
- [32] Yongqiang Qi, Shuai Li, Yi Ke, "Three-Dimensional Path Planning of Constant Thrust Unmanned Aerial Vehicle Based on Artificial Fluid Method", *Discrete Dynamics in Nature and Society*, vol. 2020, Article ID 4269193, 13 pages, 2020.
- [33] Zhang G, Zhu N, Ma S, Xia J., (2021), Humanitarian relief network assessment using collaborative truck-and-drone system, *Transportation Research Part E: Logistics and Transportation Review*, vol. 152, ISSN 1366-5545, pp. 102417, England;
- [34] Zhen L., (2015), Tactical berth allocation under uncertainty, *European Journal of Operational Research*, vol. 247, no. 3, ISSN 0377-2217, pp. 928-944, Netherlands;
- [35] Zhen L, Zhuge D, Wang S, Wang K., (2017), Daily berth planning in a tidal port with channel flow control, *Transportation Research Part B: Methodological*, vol. 106, ISSN 0191-2615, pp. 193–217.